EasyChair Preprint

№ 15979

Stability Evaluation of Thin-Walled Steel Tubular Bridge Piers under Cyclic In-Plane Eccentric Lateral and Constant Axial Loading

Iraj Hossein Pouli Mamaghani and Redeat Kassaye

July 3, 2025

Bridge Engineering Institute Conference 2025 (BEI-2025)
Paris, France, July 21-24, 2025

Stability Evaluation of Thin-Walled Steel Tubular Bridge Piers under Cyclic In-Plane Eccentric Lateral and Constant Axial Loading

Mamaghani[1*] and Redeat Kassaye[2]

[1]: Associate Professor, Grand Forks, USA; iraj.mamaghani@und.edu
[2]: PhD Student, Grand Forks, USA; redeat.kassaye@und.edu
[*]: corresponding author

Keywords: Steel, Eccentric Cyclic loading, Bridge piers, Buckling, Strength, Ductility

Abstract: This study examines the structural response of these columns under cyclic lateral loading combined with constant axial force, emphasizing ultimate strength, ductility, and the influence of load eccentricity. An elastoplastic finite element analysis was conducted to evaluate the behavior of eccentrically loaded columns. Results indicate that increasing the eccentricity reduces load capacity on the eccentric side while enhancing it on the opposite side. When the eccentricity remains within 40% of the pier height, the buckling patterns are comparable to those of centrally loaded columns. These findings offer valuable insights into the seismic performance and design optimization of thin-walled steel tubular bridge piers.

1. Introduction

Thin-walled steel tubular bridge piers—both with and without longitudinal and transverse stiffeners—are commonly used in modern highway bridge systems due to their high strength and torsional rigidity. These piers are typically configured as cantilever columns or planar rigid frames (Goto et al., 2006). Despite their advantages, such structures are prone to damage from local and global interaction, buckling under severe seismic loading. This vulnerability is primarily attributed to the high radius-to-thickness ratio (R_t) in circular sections (Nishikawa et al., 1996).

In practical design and ductility evaluation, two critical parameters for thin-walled steel hollow columns are the radius-to-thickness ratio (R_t) for circular sections and the slenderness ratio (λ) of the column (Mamaghani, 2006). The R_t ratio influences local buckling, while λ governs overall (global) stability (Usami et al., 1995). These parameters are defined using the following variables:

$$R_t = \frac{r}{t}\sqrt{3(1-v^2)}\frac{\sigma_y}{E} \quad \text{(for circular section)} \tag{1}$$

$$\lambda = \frac{2h}{r_g}\frac{1}{\pi}\sqrt{\frac{\sigma_y}{E}} \quad (2)$$

in which, b = flange width; t = plate thickness; σ_y = yield stress; E = Young's modulus; v = Poison's ratio; r = radius of the circular section; h = column height; r_g = radius of gyration of the cross-section.

The lateral yield load capacity, H_y, is governed by the minimum of the yield load, local buckling load, and overall instability load, and is evaluated using the following equations (Usami, 1996):

$$\frac{P}{P_u} + \frac{0.85H_y h}{M_y\left(1-\frac{P}{P_E}\right)} = 1 \quad (6)$$

$$\frac{P}{P_u} + \frac{H_y h}{M_y} = 1 \quad (7)$$

Where: P = the axial load; P_y = the yield load; P_u = the ultimate load; and P_E = the Euler load.

Following the damage observed in steel bridge piers during the Kobe earthquake and supported by extensive testing, a key challenge in seismic design and retrofit is improving ductility without significantly compromising the ultimate strength of the columns.

A comprehensive understanding of the cyclic inelastic behavior of thin-walled steel tubular columns is therefore essential for the development of rational, performance-based seismic design methodologies. This study investigates the behavior of thin-walled steel columns subjected to constant concentric and eccentric axial compression combined with cyclic in-plane and out-of-plane lateral loads. Nonlinear finite element analyses were performed using ABAQUS (2016). Several specimens with different geometries and eccentricities were modeled and analyzed under varying loading conditions. The analytical results were evaluated by comparing the hysteretic response curves and examining the deformation patterns of each model.

2. **Numerical Model Validation**

As shown in Figure 1, the analytical model of an eccentrically loaded column is simplified by representing the eccentric axial load, P, as a concentric load combined with an equivalent bending moment, M_0. This approach allows for more straightforward analysis while preserving the essential effects of eccentricity. The finite element results, accounting for both the material and geometrical nonlinearities (Mamaghani 1996), are validated against experimental data reported by Gao et al. (2000), confirming the reliability of the cyclic elastoplastic large-displacement analysis procedure implemented in ABAQUS.

Key variables include: R_t = radius-thickness ratio of cross section; λ= column slenderness ratio;

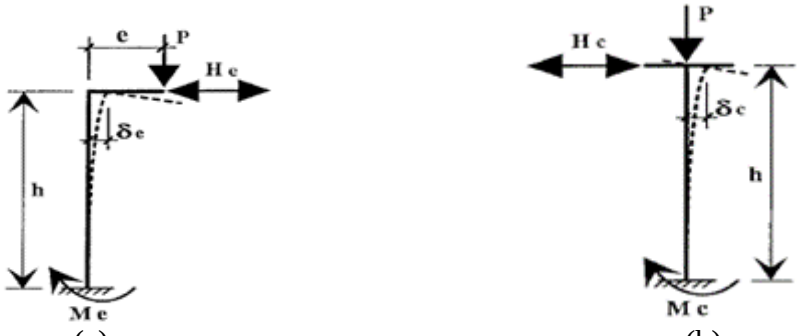

(a) (b)

Fig. 1. (a) Eccentrically Loaded Column; (b) Centrally Loaded Column

h = column height; D = diameter of circular (pipe) section; t = wall thickness; and e = eccentricity distance. The eccentricity distance e varies from 0 to 0.5h, where $e = 0$ denotes a concentrically loaded column. In all cases, the applied axial force P is set at $0.15P_\gamma$ (where P_γ is the squash load), except for the P1 series specimens, for which P is $0.12P_\gamma$.

2.1 *Finite Element Discretization of Bridge Piers*

To model the reference specimen a four-node, quadrilateral, reduced integration shell elements (S4R) were used for the tubular column with circular sections (ABAQUS, 2016). The top and bottom stiffening plates were modeled with a four-node 3-D rigid quadrilateral R3D4 element.

The finite element modeling of the tubular column is shown in Figure 2a. For thin-walled steel columns, local buckling always occurs near the base of the columns. Therefore, a coarse mesh discretization is employed for the upper part of the column, while a finer mesh discretization is adopted for the lower part of the column to consider the effect of local buckling, see Figure 2b. The length from the base, which equals the radius of the column, is divided into 15 segments, while the following length of the column is divided into 30 segments along the column length. In the circumferential direction, both meshing patterns consist of 20 segments. Adopting these two different meshing patterns reduces the computation time and required memory space in the analysis.

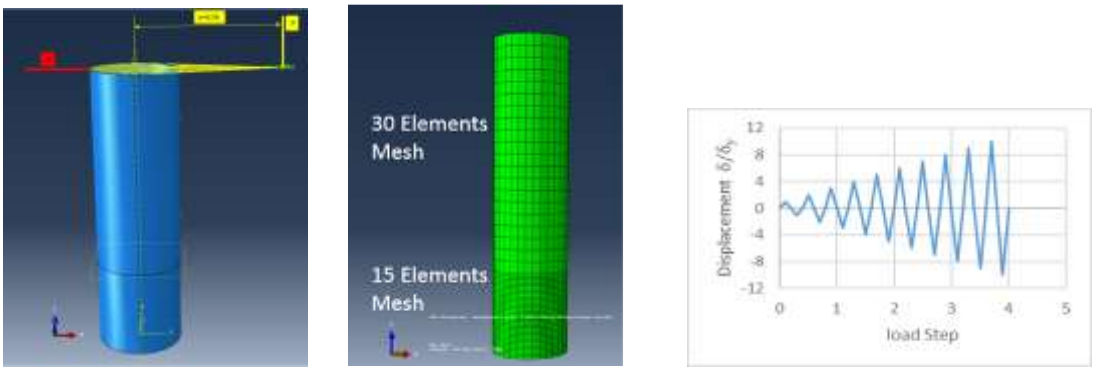

(a) (b) (c)

Fig. 2. Modelling of the analyzed column: (a) Eccentrically in-plane loading; (b) Meshing details, (c) Lateral cyclic loading

The tubes are made of JIS SS400 mild steel (equivalent to ASTM A36). The multilinear kinematic hardening material model is used in the analysis as it predicts material behavior better than the isotropic hardening material model (Mamaghani, 1996; Banno et al., 1998).

3. **Numerical Results**

Finite element analysis and experimental results for normalized lateral load (H/H_y) versus normalized lateral displacement (δ/δ_y) were plotted and compared. Comparisons of buckling, model stress distribution, and deformation level near the base of the columns at the δ/δ_y = +8 stage for the P1 series are plotted.

Figures 3a and 3b compare the normalized lateral load versus lateral displacement between tests and FEA for two specimens, P1-e_1 and P1-e2, respectively. These comparisons validate the accuracy of the adopted FE modeling in the analysis.

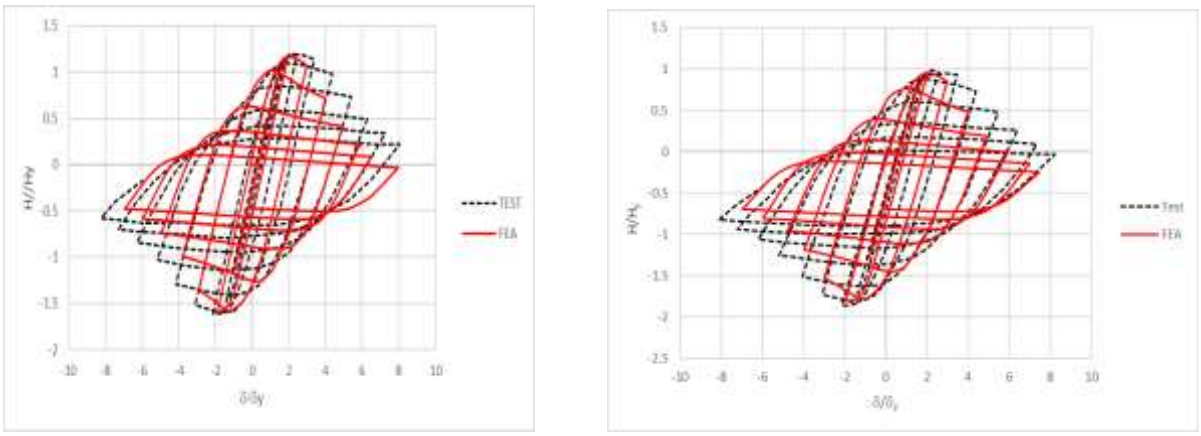

(a) (b)

Fig. 3. Comparison of Normalized Lateral Load vs. Lateral Displacement between tests (Gao et al. 2000) and FEA: (a) P1-e_1 Column; (b)P1-e2 Column.

Figure 4 compares the normalized lateral load versus lateral displacement of centrally concentric load and eccentrically concentric load, and the buckling pattern of columns near the base for the P1 series.

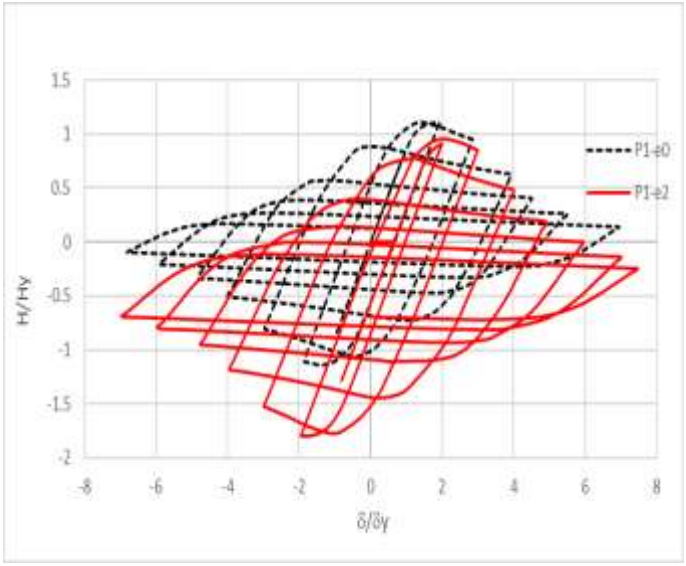

(a)

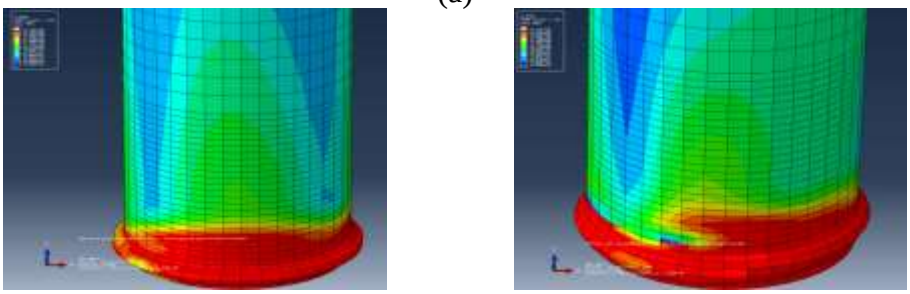

(b) (c)

Fig. 4. Comparison of Normalized Lateral Load vs. Lateral Displacement of Centrally Concentric Load and Eccentrically Concentric Load: (a) Model P1-e_0 and P1-e_2; (b) Buckling of P1-e_0, (c) Buckling of P1-e_2

From the hysteresis diagrams, it is noted that the initial structural stiffness of the eccentrically loaded column decreases with the increase in eccentric distance, mainly because of the twisting moment. From the analysis, the following observations can be made: When the eccentric distance increases, the maximum strength and ductility capacity of the eccentrically loaded columns decrease. But, deteriorations in both strength and ductility are relatively small in the case of e =0.1h. A large difference in strength and ductility is observed in the cases of e = 0.2h and e = 0.3h. It should also be noted that the initial structural stiffness of the eccentrically loaded column decreases with the increase in eccentric distance, mostly due to the influence of the twisting moment.

5. **Conclusion**

This study makes a significant contribution to the field of structural engineering by providing an in-depth exploration of the seismic behavior of stainless-steel bridge piers with stiffeners, a topic with limited studies. The paper emphasizes the performance of welded box-section piers under a combination of constant axial and cyclic lateral loading, which helps expand the understanding of how stainless steel performs in seismic applications. By employing a validated numerical Finite Element Model and conducting a thorough parametric study, the study identifies key design parameters—such as width-to-thickness ratio, slenderness ratio, and axial load ratio—that significantly impact seismic performance. The findings demonstrate that increasing both the width-to-thickness and slenderness ratios causes a substantial reduction in bearing capacity, with local buckling becoming more pronounced as these ratios increase. Additionally, the axial load ratio was found to have a moderate effect on performance, with a sharp drop in strength occurring when the axial load ratio exceeds 0.2. In summary, the study enhances the knowledge base of seismic behavior in stainless-steel piers and provides essential insights for improving bridge design, leading to more resilient and cost-effective infrastructure in seismic regions.

References

Abaqus/CAE User's Guide ABAQUS 2016.

Banno, S., Mamaghani, I.H.P., Usami, T., & Mizuno, E. 1998. "Cyclic elastoplastic large deflection analysis of thin steel plates," *Journal of Engineering Mechanics*, ASCE, 124(4), 363-370.

Gao, S., Usami, T., & Ge, H. 2000. "Eccentrically loaded steel columns under cyclic out-of-plane loading," *Journal of Structural Engineering*, 126(8), 974-981.

Goto, Y., Jiang, K., & Obata, M. 2006, "Stability and ductility of thin-walled circular steel columns under cyclic bidirectional loading," *Journal of Structural Engineering*, 132(10), 1621-1631.

Mamaghani, I. H. P. 1996. "Cyclic Elastoplastic Behavior of Steel Structures: Theory and Experiment," *Ph.D. Thesis*, Nagoya University, Nagoya, Japan.

Mamaghani, I.H.P. 2006. "Cyclic elastoplastic analysis and seismic performance evaluation of thin-walled steel tubular bridge piers," ASCE Structures Congress 2006, *17th Analysis and Computation Specialty Conference*, 1-13.

Nishikawa K, Yamamoto S, Natori T, Terao K, Yasunami H, Terada M. (1996). "An experimental study on improvement of seismic performance of existing steel bridge piers." J. of Struct. Engrg., JSCE 1996; 42A, 975-986 (in Japanese).

Usami, T., 1996. "Interim Guidelines and New Technologies for Seismic Design of Steel Structures", *Committee on New Technology for Steel Structures*, JSCE, Tokyo (in Japanese).

Usami, T., Suzuki, M., Mamaghani, I.H.P., and Ge, H.B., 1995. "A Proposal for Check of Ultimate Earthquake Resistance of Partially Concrete Filled Steel Bridge Piers", *Journal of Structural Mechanics and Earthquake Engineering*, JSCE, Tokyo, 525/I-33, 69-82, (in Japanese).